interval $E_n - \Delta E_n \leq E \leq E_n + \Delta E_n$, where $\Delta E_n = \frac{1}{2}(dE_n/dn)$. Here, E_n is considered as a "smooth" function of quantum number n. See U. Fano and J. W. Cooper, Rev. Mod. Phys. 40, 441 (1968), Sec. 2.4.

[21]For a qualitative understanding, Eq. (4) may be considered as an expansion of the exponential factor in Eq. (1) in an effective parameter Kr_{eff}, r_{eff} being a "transition radius" weighted by $\psi_n^* \psi_0$. For the transitions considered here, r_{eff} is much larger than it is for the transitions from the ground state; therefore Eq. (4) is slower in convergence for a given K. For further discussion on the convergence, see E. N. Lassettre, J. Chem. Phys. 43, 4479 (1965).

[22]Y.-K. Kim and M. Inokuti, to be published. The $1^1S \rightarrow 3^1D$ excitation will be discussed in this reference.

[23]P. G. Burke, J. W. Cooper, and S. Ormonde, to be published.

PHYSICAL REVIEW VOLUME 181, NUMBER 1 5 MAY 1969

Measured Absolute Cross Sections for K* + Rb Collisional Excitation Transfer*

Michael H. Ornstein† and Richard N. Zare‡

Department of Physics and Astrophysics, Joint Institute for Laboratory Astrophysics, University of Colorado, Boulder, Colorado 80302

(Received 27 January 1969)

The electronic excitation transfer processes,

$$K(^2P_{1/2}) + Rb(^2S_{1/2}) \rightarrow K(^2S_{1/2}) + Rb(^2P_{1/2}) + \Delta E$$

and

$$K(^2P_{3/2}) + Rb(^2S_{1/2}) \rightarrow K(^2S_{1/2}) + Rb(^2P_{1/2}) + \Delta E,$$

have been studied by irradiating a cell containing a nonequilibrium mixture of potassium and rubidium vapors with either the 7665 Å D2 line or the 7699 Å D1 line of the potassium resonance doublet. The resulting collisionally induced rubidium 7948 Å fluorescence signal, isolated by interference filters used in tandem, is detected with a liquid-nitrogen–cooled S-1 photomultiplier placed at right angles to the direction of excitation. Measurements of the intensity ratio of the potassium and rubidium fluoresence combined with an optical absorption determination of the rubidium atom density yields the following excitation transfer cross sections:

$$Q[K(^2P_{1/2}) \rightarrow Rb(^2P_{1/2})] = 2.2 \text{ Å}^2 \pm 25\%$$

and

$$Q[K(^2P_{3/2}) \rightarrow Rb(^2P_{1/2})] = 2.6 \text{ Å}^2 \pm 20\%$$

at $T = 365°\text{K} \pm 2\%$. Throughout an experimental run the potassium and rubidium vapor pressures are varied, but data are taken for only the lowest vapor pressures for which corrections due to resonance radiation imprisonment are unnecessary.

I. INTRODUCTION

When a gas gains energy by photo-excitation, electron impact, shock heating, radiolysis, chemical reaction, etc., appreciable concentrations of electronically excited atoms and molecules are often generated. These excited species may emit radiation, or they may be de-excited through various collisional encounters in which the energy is redistributed among the collision partners. The competition among the different deactivation pathways controls the subsequent physical behavior and chemical properties of the gas. Knowledge of the absolute cross sections (reaction rates) for energy transfer is thus of fundamental importance in understanding such diverse phenomena as flash photolysis, flames, discharges, shocks, auroras, and stellar atmospheres. Among the various types of energy transfer, those between colliding atoms in different states of excitation are, in principle, some of the simplest. Of these, the excitation transfer between different alkali atoms has been of particular interest to us not only because such systems typify a large class of near-adiabatic inelastic processes, but also because these systems, which can be treated as hydrogen-like, offer promise of allowing a critical comparison between theory and experiment. We report here an experimental study of the interchange of electronic excitation between the lowest-lying excited states of potassium and rubidium in which cross sections for energy transfer between some of the fine-

structure levels have been determined.

"Sensitized fluorescence" resulting from collisional transfer of excitation between different atoms (so-called collisions of the second kind) is easy to detect and there have been numerous experimental studies.[1-4] The standard method for studying excitation transfer is to illuminate a mixture of two gases, A and B, with radiation which only one gas, say A, can absorb and to observe the resulting fluorescence. The excited atom A^* may lose its energy directly by reradiation

$$A^* \rightarrow A + h\nu \qquad \text{(resonance fluorescence)},$$

or A^* may become de-excited through collisions in only three ways (excluding ionization):

$$A^* + B \rightarrow A + B^* \rightarrow A + B + h\nu \qquad \text{(sensitized fluorescence)},$$

$$A^* + B \rightarrow A + B \qquad \text{(fluorescence quenching)},$$

and $$A^* + B \rightarrow AB + h\nu \qquad \text{(two-body radiative recombination)}.$$

If the energy difference between B^* and A^* is small, sensitized fluorescence is the dominant atomic-collision process for energy loss.

The excited states A^* and B^* normally will show a fine-structure splitting because of spin-orbit interaction. This makes it possible to investigate the relative efficiency of energy transfer to and from the different multiplets of A^* and B^*. The presence of multiplet structure also gives rise to

TABLE I. Atomic excitation transfer studies.

Collision System	References listed in Table II
$He^* + Ne$	38, 39, 41, 51
$K^* + Rb$	34, 54
$Kr^* + Hg$	16. 19
$Rb^* + Cs$	47
$Cd^* + Cs$	36
$Hg^* + Na$	8, 9, 11, 14, 15, 21, 22, 35, 40, 42, 45
$Hg^* + K$	27
$Hg^* + Cr$	33
$Hg^* + Fe$	32
$Hg^* + Zn$	6, 10, 12, 13, 46, 55
$Hg^* + Ag$	1
$Hg^* + Cd$	2, 17, 18, 53
$Hg^* + In$	3, 30
$Hg^* + Sn$	24, 25, 31
$Hg^* + Tl$	1, 2, 3, 5, 7, 20, 23, 26, 28, 37, 43, 44, 48, 49, 50, 52
$Hg^* + Pb$	4, 29, 31
$Hg^* + Bi$	4

TABLE II. References to Table I given in chronological order.

Cross-reference to Table I

1 G. Cario, Z. Physik 10, 185 (1922).
2 G. Cario and J. Franck, Z. Physik 17, 202 (1923).
3 K. Donat, Z. Physik 29, 345 (1924).
4 H. Kopfermann, Z. Physik 21, 316 (1924).
5 S. Loria, Phys. Rev. 26, 573 (1925).
6 J. G. Winans, Proc. Natl. Acad. Sci. U.S. II, 738 (1925).
7 W. Orthmann and P. Pringsheim, Z. Physik 35, 626 (1926).
8 F. Rasetti, Nature 118, 47 (1926).
9 H. Beutler and B. Josephy, Naturwiss. 15, 540 (1927).
10 J. G. Winans, Phys. Rev. 30, 1 (1927).
11 H. Beutler, Physik Z. 29, 893 (1928).
12 J. G. Winans, Phys. Rev. 31, 710 (1928).
13 J. G. Winans, Phys. Rev. 32, 427 (1928).
14 H. Beutler and B. Josephy, Z. Physik 53, 747 (1929).
15 H. W. Webb and S. C. Wang, Phys. Rev. 33, 329 (1929).
16 H. Beutler and W. Z. Eisenchimmel, Z. Physik Chem. (Frankfurt), B10, 89 (1930).
17 A. C. G. Mitchell, J. Franklin Inst. 209, 747 (1930).
18 A. C. G. Mitchell, Phys. Rev. 35, 1422 (1930).
19 H. Beutler and W. Z. Eisenschimmel, Z. Elektrochem. 37, 582 (1931).
20 O. S. Duffendack, Phys. Rev. 37, 107 (1931).
21 A. Ferchmin and S. Frisch, Phys. Z. Sowietunion 9, 466 (1936).
22 S. E. Frisch, Izv. Akad. Nauk SSSR Ser. Fiz. 3, 431 (1936).
23 S. Mrozowski, Acta Phys. Polon. 6, 58 (1937).
24 J. G. Winans and R. W. Williams, Phys. Rev. 52, 250 (1937).
25 J. G. Winans and R. W. Williams, Phys. Rev. 52, 930 (1937).
26 J. G. Winans and F. J. Davis, Phys. Rev. 53, 930 (1938).
27 E. A. Krause, Phys. Rev. 55, 164 (1939).
28 J. G. Winans, F. J. Davis, and V. A. Leitzke, Phys. Rev. 55, 242 (1939).
29 J. G. Winans, F. J. Davis, and V. A. Leitzke, Phys. Rev. 55, 1126 (1939).
30 J. G. Winans, F. J. Davis, and V. A. Leitzke, Phys. Rev. 57, 70 (1940).
31 J. G. Winans, Phys. Rev. 60, 169 (1941).
32 J. G. Winans and S. Been, Phys. Rev. 62, 297 (1942).
33 J. G. Winans and W. J. Pierce, Phys. Rev. 64, 43 (1943).
34 M. A. Thangaraj, Ph.D. thesis, University of Toronto, Toronto, Canada, 1948 (unpublished).
35 S. E. Frisch and E. K. Kraulinya, Dokl. Akad. Nauk SSSR 101, 837 (1955).

TABLE II. (*cont.*)

36 H. Friedrich and R. Seiwert, Ann. Physik 20, 215 (1957).
37 R. A. Anderson and R. H. McFarland, Phys. Rev. 119, 693 (1960).
38 A. Javan, W. R. Bennett, Jr., and D. R. Herriott, Phys. Rev. Letters 6, 106 (1961).
39 E. E. Benton, F. A. Matson, E. E. Ferguson, and W. W. Roberts, Phys. Rev. 128, 206 (1962).
40 S. E. Frisch and O. P. Bochkova, Zh. Eksperim. i Teor. Fiz. 43, 331 (1962) [English transl.: Soviet Phys. – JETP 16, 237 (1963)].
41 A. B. White and E. I. Gordon, Appl. Phys. Letters 3, 197 (1963).
42 E. K. Kraulinya, Opt. i Spektroskopiya 17, 464 (1964) [English transl.: Opt. Spectry. (USSR) 17, 250 (1964)].
43 E. E. Step and R. A. Anderson, Phys. Letters 11, 127 (1964).
44 E. K. Kraulinya, A. E. Lezdin, and Yu. A. Silin, Opt. i Spektroskopiya 19, 154 (1965) [English transl.: Opt. Spectry. (USSR) 19, 84 (1965)].
45 S. G. Rautian and A. S. Khaikin, Opt. i Spektroskopiya 18, 722 (1965) [English transl.: Opt. Spectry. (USSR) 18, 406 (1965)].
46 M. L. Sosinskii and E. N. Morozov, Opt. i Spektroskopiya 19, 634 (1965) [English transl.: Opt. Spectry. (USSR) 19, 352 (1965)].
47 M. Czajkowski, D. A. McGillis, and L. Krause, Can. J. Phys. 44, 741 (1966).
48 B. C. Hudson and B. Curnutte, Jr., Phys. Rev. 148, 60 (1966).
49 B. C. Hudson and B. Curnutte, Jr., Phys. Rev. 152, 56 (1966).
50 E. K. Kraulinya and A. E. Lezdin, Opt. i Spektroskopiya 20, 539 (1966) [English transl.: Opt. Spectry. (USSR) 20, 304 (1966)].
51 O. P. Bochkova, Yu. A. Tolmachev, and S. E. Frisch, Opt. i Spektroskopiya 23, 500 (1967) [English transl.: Opt. Spectry. (USSR) 23, 270 (1967)].
52 C. F. Gallo, Phys. Rev. 158, 1 (1967).
53 W. Gough, Proc. Phys. Soc. (London) 90, 287 (1967).
54 M. H. Ornstein, J. K. Link, and R. N. Zare, Bull. Am. Phys. Soc. 12, 1147 (1967).
55 M. L. Sosinskii and E. N. Morozov, Opt. i Spektroskopiya 23, 868 (1967) [English transl.: Opt. Spectry. (USSR) 23, 475 (1967)].

a closely related energy transfer process[4,5] in which collisions with A^* induce transitions between the components of its multiplets:

$$A_J^* + M \rightarrow A_{J'}^* + M \quad \text{(intramultiplet conversion)},$$

where M is A or B. In distinction, sensitized fluorescence, resulting from the transfer of excitation from the multiplet levels of A^* to those of B^* may be viewed as "intermultiplet conversion."

In Tables I and II we have collected all known references to experimental studies of excitation transfer between different atoms. Sensitized fluorescence was first reported in 1922 by Cario, a student of Franck, who irradiated a mixture of mercury and thallium vapor with the mercury 2537 Å resonance line. The gases were contained in a bulb placed inside an oven such that the pressure of the mercury vapor was 0.25 mm, and of the thallium vapor 2 mm. Under these conditions the fluorescence spectrum consisted, apart from the mercury resonance line, of a large number of thallium lines. In much the same way, sensitized fluorescence was later obtained in the vapors of sodium, potassium, cadmium, indium, lead, and silver, always with Hg^* as the sensitizer. The next advance was due to Winans and his co-workers. They devised an ingenious method for exciting sensitized fluorescence in the vapors of the more refractory metals. The metal is crushed to a fine powder, placed inside a sealed quartz tube containing mercury, and heated by torch to the highest temperature the tube walls will withstand without collapsing. This procedure expanded the list of elements whose fluorescence spectrum had been observed to include zinc, tin, iron, and chromium. From Tables I and II, it can be seen that from about 1940–1960 there was little progress. Recent developments such as the He-Ne laser, which uses excitation transfer to obtain population inversion,[6] have rekindled interest in this field and have provided us with perhaps the most quantitative information to date. In view of the total number of investigations listed in Tables I and II, it seems quite remarkable that almost all known sensitized fluorescence studies of metal vapors have involved energy transfer with mercury.

The interpretation of mercury photosensitized fluorescence has seldom been clear cut and a critical examination of efforts in the past will illustrate the difficulties associated with making quantitative measurements of excitation transfer. The excited Hg^* atoms, possessing 4.48 eV above the ground state, normally transfer their electronic energy to high-lying atomic levels of other elements, producing a complex fluorescence spectrum due to radiative cascade. The various oscillator strengths are seldom known for transitions from these levels and it is often difficult to determine which states have been directly excited. Furthermore, at these excitation energies chemi-ionization may become an important pathway. For example, in the $Hg^* + K$ system the ionization potential of potassium is below the electronic energy of Hg^*. The use of the unfiltered output from a mercury resonance lamp often further complicated the explanation. Since the vapor pressures are usually about 1 mm and seldom less

than 0.001 mm, step-wise excitation, reabsorption and imprisonment of resonance radiation as well as fluorescence quenching can play a significant role. There is also some question whether the 1849 Å resonance line, exciting mercury atoms to the $^1P_1$ level, might be responsible for excitation transfer. It is believed to contribute appreciably to the fluorescence observed in zinc vapor. The first studies of Hg* + Tl by Cario and Franck were performed under these poorly defined conditions. In 1931, Duffendack replaced the water-cooled mercury arc with a hot mercury light source whose 2537 Å line was self-reversed; the thallium fluorescence was observed to disappear. However, in 1937 Mrozowski demonstrated that the thallium fluorescence spectrum could be produced by primary excitation of the Hg_2 molecules in the vapor. Mercury readily amalgamates with other metals and it is not uncommon for molecular fluorescence bands to be observed. This presents another difficulty. The vapor pressures of the atomic vapors over the amalgam cannot be assumed to be the same as the vapor pressures of the pure metals at the same temperature. Finally it is important to note that Hg* may be converted upon collision to the metastable Hg $^3P_0$ state. This is favored at high pressures or upon addition of a foreign gas such as N_2 or O_2. Sensitized fluorescence resulting by energy transfer from this state has seldom been separated from that produced by the short-lived Hg $^3P_1$ state. These considerations point up some of the experimental pitfalls which must be avoided in attempting quantitative measurements of atomic excitation transfer.

Although sensitized fluorescence has long been studied, determinations of absolute values for the cross sections have only been reported recently for the Hg* + Na, Hg* + Zn, Hg* + Tl, Cd* + Cs, and Rb* + Cs collision systems. In all of these studies serious questions can be raised regarding the reliability of the measured cross sections due to possible systematic errors. We present here an experimental study of the K* + Rb collision system. We have attempted to understand and control the possible sources of systematic errors and to make quantitative estimates of the uncertainty they contribute to our measured cross sections. Because of the difficulties involved in making absolute measurements, we place special emphasis on consistency checks and other experimental tests which were used to ensure the reliability of our measurements.

II. RELATION BETWEEN EXPERIMENTAL OBSERVABLES AND THE CROSS SECTION

The present investigation is a study of the photosensitized reaction

$$K(^2P_J) + Rb(^2S_{\frac{1}{2}}) \rightarrow K(^2S_{\frac{1}{2}}) + Rb(^2P_{J'}) + \Delta E \ , \qquad (1)$$

whereby electronic excitation is exchanged between the lowest-lying excited states of potassium and rubidium during a binary encounter. Figure 1 gives a schematic energy-level diagram of the states involved. It illustrates the processes which result when a cell containing a mixture of potassium and rubidium vapors is irradiated with the D2 component of the potassium resonance doublet. The potassium and rubidium fine-structure levels $^2P_{1/2}$ and $^2P_{3/2}$ are labeled by the indices 1 and 2, respectively. The resulting fluorescence contains primarily the direct resonance fluorescence of the exciting potassium D2 line, as well as weak lines arising from a number of collisional energy transfer processes between excited and unexcited K atoms, excited K atoms and unexcited Rb atoms, and excited and unexcited Rb atoms.

In treating these collision processes, we will use the following simple notation: N_{Rb} for the Rb ground-state atom density, N_i^{Rb} for the Rb ith excited-state atom density, τ_i^{Rb} for the Rb ith excited-state radiative lifetime, and I_i^{Rb} for the Rb ith excited-state fluorescence intensity

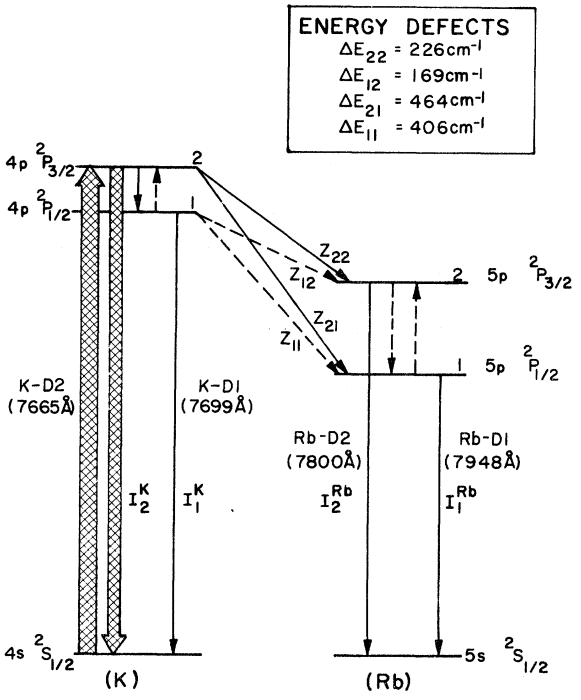

FIG. 1. Schematic energy-level diagram indicating the energy transfer processes when a mixture of K and Rb vapor is irradiated with K-D2 light. Arrows terminating on the ground state indicate spontaneous decay. All others, except the pumping light, represent collisional excitation transfers. Dashed lines signify secondary collisional transfers.

(photons per second emitted per unit volume); with a similar set of designations for potassium. A subscript $i = 1$ or 2 is added to the symbols N^{Rb}, τ^{Rb}, and I^{Rb} to indicate the $^2P_{1/2}$ or $^2P_{3/2}$ level, respectively, for the excited state.

Under our experimental conditions ($N_K \lesssim 5\times10^{10}$ atoms/cm^3, $N_{Rb} \sim 5\times10^{11}$ atom/cm^3), a number of the transfer processes indicated in Fig. 1 can be shown to be negligible, resulting in a simple relation between the Rb sensitized fluorescence and the direct K resonance fluorescence,

$$I_1^{Rb} = I_2^{K} Q_{21} \bar{v} \tau_2^{K} N_{Rb}. \tag{2}$$

Here Q_{21} is the Maxwell-Boltzmann averaged cross section for transfer from K in level 2 to Rb in level 1, and

$$\bar{v} = (8kT/\pi\mu)^{1/2} \tag{3}$$

is the mean relative velocity between the collision partners. In Eq. (3), T is the absolute temperature of the gas mixture, k is the Boltzmann constant, and μ is the reduced mass. The radiative lifetime of the excited K atom is well known[7] ($\tau = 2.78\times10^{-8}$ sec). The absolute cross section Q_{21} may thus be determined by measuring (a) the absolute temperature T of the cell, (b) the rubidium ground-state atom density, and (c) the I_1^{Rb}/I_2^{K} fluorescence intensity ratio.

The derivation of Eq. (2) proceeds as follows. Under our experimental conditions, the ratio of Rb sensitized fluorescence to K resonance fluorescence was less than one part in 10^6. Intramultiplet conversion for $K\,^2P_{1/2} \rightleftharpoons K\,^2P_{3/2}$ has been studied by Chapman and Krause[8] and for $Rb\,^2P_{1/2} \rightleftharpoons Rb\,^2P_{3/2}$ by Rae and Krause[9] who have reported cross sections on the order of 300 Å^2 and 50 Å^2, respectively. Relative to the excitation transfer process $K\,^2P_{3/2} \rightarrow Rb\,^2P_{1/2}$, shown by the solid arrow in Fig. 1, all collision processes shown by dashed arrows thus contribute less than one part in 10^5 to the collisional population or depopulation of the $Rb\,^2P_{1/2}$ level at the low pressures we employed. For the collision process shown in Fig. 1 the (steady-state) rubidium fluorescence intensity I_1^{Rb} is thus given by

$$I_1^{Rb} = N_2^{K} Z_{21}, \tag{4}$$

where Z_{21} is the collision transfer rate, defined as the number of transfers per second per excited K atom in level 2 to Rb atoms in level 1. It is traditional to write Z_{21} in terms of a Maxwell-Boltzmann averaged cross section $Q_{21}(T)$ by

$$Z_{21} = Q_{21}(T)\bar{v} N_{Rb}. \tag{5}$$

The cross section $Q_{21}(T)$ defined in this manner is actually an average of the velocity-dependent cross section $\sigma_{21}(v)$ weighted by the relative velocity distribution function $F(v, T)$,

$$Q_{21}(T) = \frac{\int_0^\infty F(v,T)\sigma_{21}(v)v\,dv}{\int_0^\infty F(v,T)v\,dv}. \tag{6}$$

The excited-state potassium atom density may be expressed in terms of the radiative lifetime of the state by

$$N_2^{K} = I_2^{K} \tau_2^{K}. \tag{7}$$

If we substitute Eqs. (5) and (7) into Eq. (4) we obtain Eq. (2).

It should be noted that the above derivation is strictly valid only when the cell is optically thin to both K and Rb resonance radiation. Of the two, the optical depth of potassium is more critical. If the K radiation is trapped by reabsorption, the calculation of the cross section is affected in two ways: (1) by the change in the effective value of the radiative lifetime of the potassium excited state, and (2) by the change in the I_1^{Rb}/I_2^{K} fluorescence ratio due to the angular distribution of the fluorescence. The former is the more significant way. When the potassium resonance radiation is imprisoned, the effective number of excited K atoms transferring excitation to Rb, N_2^{K} in Eq. (4) can be much larger than the value of N_2^{K} given by Eq. (7), which is the product of the measured K fluorescence intensity times the K atom radiative lifetime. This increases the effective lifetime of K photons and causes I_1^{Rb} to exceed the value calculated from Eq. (2).

Under conditions of radiation trapping the resultant fluorescence is anisotropic and depends on the geometry of the cell. If fluorescent light is collected over all 4π sr, the ratio I_1^{Rb}/I_2^{K} is unaffected provided the radiation trapping is not so severe as to cause appreciable alteration of the intensities from excitation transfer processes. However, if the fluorescence intensity ratio I_1^{Rb}/I_2^{K} is measured by a detector subtending a finite solid-angle element of the cell, radiation trapping will cause an apparent change in the I_1^{Rb}/I_2^{K} ratio. In contrast to K radiation trapping, this is the only way Rb radiation trapping can affect the cross-section determination. In our experimental investigations the K radiation was not trapped and the Rb density was varied from 5×10^{10} atoms/cm^3 to 1×10^{12} atoms/cm^3. In the lower density region the optical depth of the Rb resonance radiation was much less than 1, but at the higher densities the optical depth increased to about 2, and the Rb radiation was becoming trapped. The effects of such radiation imprisonment on the ratio I_1^{Rb}/I_2^{K} were further minimized by using a cell of cylindrical geometry and collimating the exciting beam so that it passed through

the center of the cell.[10]

III. THE DENSITY MEASUREMENT

A. Theory

In determining the absolute cross section in sensitized fluorescence experiments such as this, a major source of difficulty is the reliable measurement of the ground-state density of the atom to which transfer is made. In similar experiments the vapor-pressure curve versus temperature has been used, assuming that the accurately known temperature of the coolest part of the cell (usually a side arm containing a pool of metal) determines the vapor pressure in the main body of the cell.[4] We have found (as have others)[5,7,11,12] that this method is questionable due to saturation effects, whereby the alkali metals seem to diffuse in and out of the glass walls of the cell, making the actual vapor pressure a complicated function of the entire cell, its history, and the time allowed for equilibration. Besides, the vapor pressure data of a potassium-rubidium amalgam are unknown. To overcome these problems we have determined the rubidium density by an optical absorption method, outlined as follows.

When a beam of Rb resonance radiation with frequency spectrum $i_0(\nu)$ is passed through a length l of absorbing Rb vapor, the transmitted radiation is given by the well-known expression[1]

$$i(\nu) = i_0(\nu) \exp[-k(\nu, N_{\mathrm{Rb}})l], \tag{8}$$

where $k(\nu, N_{\mathrm{Rb}})$ is the absorption coefficient which depends on the ground-state atom density. We define

$$I_0 = \int_{-\infty}^{\infty} i_0(\nu)d\nu, \tag{9}$$

$$I = \int_{-\infty}^{\infty} i(\nu)d\nu \tag{10}$$

and

$$A = (I_0 - I)/I_0 \tag{11}$$

where I_0 is the total incident intensity, I is the total transmitted intensity, and A is the absorption. If we substitute Eqs. (8)–(10) into Eq. (11), we obtain

$$A(N_{\mathrm{Rb}}) = \frac{\int_{-\infty}^{\infty} i_0(\nu)[1 - e^{-k(\nu, N_{\mathrm{Rb}})l}]d\nu}{\int_{-\infty}^{\infty} i_0(\nu)\,d\nu}. \tag{12}$$

The quantity A is readily measured in the laboratory; hence from a knowledge of l and the functions $i_0(\nu)$ and $k(\nu, N_{\mathrm{Rb}})$, the density N_{Rb} can be determined from the absorption measurement using a simple computer program which performs the integrals in Eq. (12) to obtain A as a function of N_{Rb}.

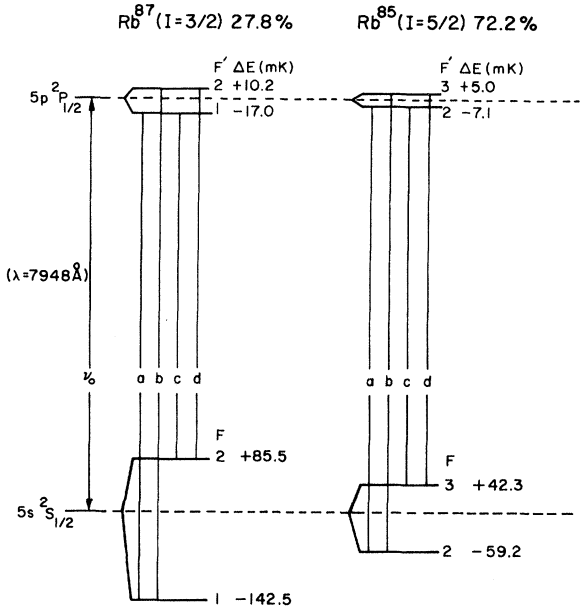

FIG. 2. Hyperfine structure of the ground state and first excited state of rubidium. Splittings from the center of gravity are given in mK = 10^{-3} cm^{-1}. Natural isotopic abundances are assumed.

An important problem encountered in such measurements is the line profile of the light beam. One is seldom sure how broadened or even self-reversed the resonance lines originating from a lamp may be. Others[12–14] have resorted to complicated Fabry-Perot measurements in attempting to settle this question, however, the Fabry-Perot instrumental width is a source of much concern in interpreting such measurements. We believe we have largely circumvented these difficulties by using a Rb vapor fluorescence cell placed in front of a Rb lamp (see experimental setup, Sec. III, B). The fluorescent lines which emerge from the Rb fluorescence cell at right angles to the lamp-beam direction have a profile which is independent of the line profile of the lamp beam.[15] For Rb vapor densities in which the optical depth of the emitted radiation is much less than unity, the emitted resonance lines have a profile whose functional dependence on ν is the same as that of the absorption coefficient.

Under the conditions of our experiment the emitted resonance lines have a pure Doppler profile determined by the temperature of the Rb fluorescence cell. It is this fluorescent light which is passed through the main cell (containing K and Rb vapor) in the density determination. A noteworthy feature of this method is that the temperature determination of the main cell and of the Rb fluorescence cell is not critical, entering essentially only through the Doppler widths, proportional to

$T^{1/2}$ (e.g., a change from 100 to 120°C in the temperature of the Rb cell body causes less than a 2% change in the value of N_{Rb} determined from the computed curve of A versus N_{Rb}).

The 7948 Å D1 rubidium resonance line, selected by an interference filter (which transmitted less than 0.1% of the 7800 Å rubidium D2 line) is used in the density measurement. Some complications arise owing to the presence of the two naturally occurring isotopes, $Rb^{85}(I = \frac{5}{2})$ and Rb^{87} $(I = \frac{3}{2})$, in the lamp, the Rb cell and the main cell. Figure 2 shows the resultant hyperfine structure (hfs) whereby the Rb-D1 line splits into eight components, four for each isotope. In Fig. 2 the ground-state splittings (in mK = 10^{-3} cm^{-1}) are taken from Bederson and Jaccarino[16] and the excited-state splittings from Senitsky and Rabi.[17] The Rb ground-state isotope shift is quoted by Kopfermann and Krüger[18] as 0.000 ± 0.002 cm^{-1} and henceforth will be ignored.

The radiation which emerges from the Rb fluorescence cell at right angles to the direction of the lamp beam consists of a series of Doppler-broadened hfs components whose relative intensities depend upon the population of the excited-state hfs levels in the Rb fluorescence cell. The populations of these levels are determined, in turn, by the details of the lamp profile, thus making the absorption measurement still somewhat dependent on lamp conditions. However, we have found both experimentally and theoretically that the absorption A is quite insensitive to a wide range of lamp conditions, giving us confidence in the validity of this technique as a means of making accurate density determinations.

The mathematical formulation of the density-measurement method proceeds as follows. For the the ith hfs component centered about the frequency ν_i (in cm^{-1}), the absorption coefficient is

$$k_i(\nu) = \kappa_i \exp[-(\nu - \nu_i)^2/\Delta\nu_i^2] , \tag{13}$$

where $$\Delta\nu_i = [2kT/M_i c^2]^{1/2}\nu_i \tag{14}$$

is the Doppler width (defined as the half-width at the value for which the Doppler profile is e^{-1} of its maximum). In Eq. (14), c is the velocity of light (cm/sec) and M_i is the mass (g) of the Rb^{85} or Rb^{87} isotope. Integration of Eq. (13) over frequency gives

$$\int_{-\infty}^{\infty} k_i(\nu)\,d\nu = \kappa_i \pi^{1/2} \Delta\nu_i . \tag{15}$$

This expression may be related to the familiar[1] absorption f value for the transition of the i th component of the hfs by

$$\int_{-\infty}^{\infty} k_i(\nu)\,d\nu = \pi r_0 f_i N_i , \tag{16}$$

where $r_0 = 2.82 \times 10^{-13}$ cm is the classical electron radius and N_i is the population of the lower-state hfs level for the ith transition. From Eqs. (15) and (16) we find that

$$\kappa_i = \pi^{1/2} r_0 N_i f_i / \Delta\nu_i . \tag{17}$$

Denoting βi as the inverse of the Doppler width [defined in Eq. (14)] of the ith hfs component in the main cell in which the Rb density is to be determined, we obtain for the total absorption coefficient the expression

$$k(\nu) = \sum_{i=1}^{8} \kappa_i e^{-\beta_i^2(\nu - \nu_i)^2} . \tag{18}$$

Similarly, by denoting α_j as the inverse of the Doppler width of the jth hfs component in the Rb cell, we obtain for the line profile of the radiation emerging from the Rb fluorescence cell

$$i_0(\nu) = \sum_{j=1}^{8} i_0(j)\pi^{-\frac{1}{2}} \alpha_j e^{-\alpha_j^2(\nu - \nu_j)^2} , \tag{19}$$

where $i_0(j)$ is the total intensity of the jth hfs component. Substituting Eqs. (18) and (19) into Eq. (12), we find

$$A = \int_{-\infty}^{\infty} d\nu \sum_{j=1}^{8} \frac{i_0(j)}{i_0(1)} \alpha_j e^{-\alpha_j^2(\nu - \nu_j)^2} \times \left[1 - \exp\left(-\sum_{i=1}^{8} C_i e^{-\beta_i^2(\nu - \nu_i)^2}\right)\right] \times \left(\int_{-\infty}^{\infty} d\nu \sum_{j=1}^{8} \frac{i_0(j)}{i_0(1)} \alpha_j e^{-\alpha_j^2(\nu - \nu_j)^2}\right)^{-1} , \tag{20}$$

where $C_i = \pi^{1/2} r_0 l \beta_i N_i f_i$. We proceed to determine the values of f_i, N_i, and the relative intensity ratios $i_0(i)/i_0(1)$ required to evaluate Eq. (20).

To find the f values for the eight hfs transitions shown in Fig. 2, we use the expressions

$$f_{F \to F'} = \gamma(2F' + 1)[W(\tfrac{1}{2} F' \tfrac{1}{2} F; I1)]^2 \tag{21}$$

and

$$(f_a + f_b)_{85 \text{ or } 87} = (f_c + f_d)_{85 \text{ or } 87} = f_{\text{tot}} . \tag{22}$$

In Eq. (21) γ is the same for all transitions between the $5s\,^2S_{1/2}$ and $5p\,^2P_{1/2}$ levels, W is a Racah coefficient, and F and F' are the total angular momentum quantum numbers for the lower and upper states, respectively. The notation a, b, c, d in Eq. (22) refers to Fig. 2 and f_{tot} is the ab-

TABLE III. The f values for Rb-D1 hyperfine transitions shown in Fig. 2.

Isotope	f_a	f_b	f_c	f_d
Rb^{85}	0.0744	0.261	0.186	0.149
Rb^{87}	0.0558	0.279	0.168	0.168

sorption f value, equal to 0.335, for the D1 line.[7] The derivation of Eqs. (21) and (22) is presented in the Appendix. The hfs f values obtained from Eqs. (21) and (22) are given in Table III.

The populations of the ground-state hfs levels, N_F^{85}, are related to the total ground-state density, N^{85}, for Rb^{85} by

$$N_F^{85} = N^{85}(2F+1)/\sum_F (2F+1)\,, \tag{23}$$

with a similar expression for Rb^{87}. Assuming natural isotopic abundances,[19]

$$N^{85} = 0.722 N_{\mathrm{Rb}} \tag{24a}$$

and

$$N^{87} = 0.278 N_{\mathrm{Rb}}, \tag{24b}$$

where N_{Rb} is the total ground-state density, the determination of which is the purpose of this part of the experiment.

The $i_0(j)/i_0(1)$ relative intensity ratios depend on the relative upper-state hfs populations in the Rb cell, and as pointed out earlier, it is only here that the lamp conditions play a role. To estimate the magnitude of their effect on the absorption measurement, both theoretical and experimental checks were carried out. The intensity of the jth component in $i_0(\nu)$ is related to the transition probability per sec $A_{F'(j)\to F(j)}$ by

$$i_0(j) = N_{F'(j)} A_{F'(j)\to F(j)}. \tag{25}$$

It follows then from standard Racah techniques that the intensity ratio is given by[20]

$$\frac{i_0(j)}{i_0(1)} = \frac{N_{F'(j)}[2F(j)+1]}{N_{F'(1)}[2F(1)+1]} \times \left(\frac{W(\tfrac{1}{2}F'(j)\tfrac{1}{2}F(j);I(j)1)}{W(\tfrac{1}{2}F'(1)\tfrac{1}{2}F(1);I(1)1)} \right)^2 . \tag{26}$$

The ratios of the hfs populations $N_{F'(j)}/N_{F'(1)}$ in Eq. (26) are determined by the lamp profile $I(\nu)$. Under steady-state excitation the relative populations can be derived[20] from the expression

$$dN_{F'}^{85}/dt = 0 = \int d\nu \sum_j N_{F(j)}^{85}(\nu)\, B_{F(j)\to F'}^{85} I(\nu) - N_{F'}^{85}/\tau^{\mathrm{Rb}}(D1)\,, \tag{27}$$

where $N_{F(j)}^{85}(\nu)$ is the number of atoms in the lower state of the jth transition capable of absorbing light in the frequency interval ν to $\nu + d\nu$, and B is the Einstein absorption coefficient for the transition. The summation in Eq. (27) is over the two hfs transitions connecting the ground state to F' for Rb^{85}. A similar expression can be used for Rb^{87}.

To investigate how the lamp profile might affect the final absorption measurement, we calculated $A(N_{\mathrm{Rb}})$ for the following different physically reasonable assumptions:

(a) The lamp profile consists of a series of Doppler profiles arising from assumed statistical populations of the excited states in the lamp, with natural isotopic abundances. The Doppler width in the lamp is varied from 1 to 4 times the Doppler width in the Rb cell.

(b) The lamp profile consists of a series of Doppler profiles all of equal intensity for a given isotope, but between isotopes the intensities are in the ratio of the isotopic abundances. The Doppler width is varied again from 1 to 4 times the Doppler width in the Rb cell.

Cases (a) and (b) together cover a considerable range of broadening as well as incipient self-reversal. Equations (26) and (27) in conjunction with a simple computer program were used to cal-

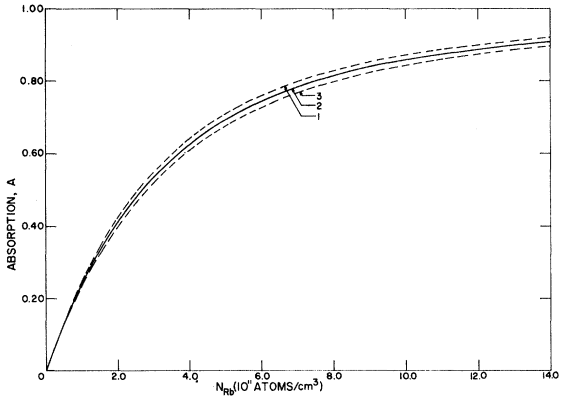

FIG. 3. Calculated absorption curves for Rb-D1 light passing through a 1-cm path length of Rb vapor in the main cell with the experimental setup shown in Fig. 4. Dashed curves indicate extremes for the various Rb-lamp conditions discussed in the text. Curve 1 corresponds to case (b), line 1 of Table IV, and curve 3 corresponds to case (a), line 4 of Table IV. Curve 2 represents the mean of curves 1 and 3.

TABLE IV. Relative intensity ratios of the hfs components for the Rb-D1 line.

Doppler widths in lamp	I_a^{85}	I_b^{85}	I_c^{85}	I_d^{85}	I_a^{87}	I_b^{87}	I_c^{87}	I_d^{87}
				Case (a)				
$1\times\Delta\nu_{\text{cell}}$	0.286	0.935	1.000	0.748	0.019	0.118	0.096	0.118
$2\times\Delta\nu_{\text{cell}}$	0.286	0.871	1.000	0.697	0.021	0.152	0.104	0.152
$3\times\Delta\nu_{\text{cell}}$	0.286	0.841	1.000	0.672	0.027	0.192	0.136	0.192
$4\times\Delta\nu_{\text{cell}}$	0.286	0.831	1.000	0.665	0.036	0.216	0.182	0.216
				Case (b)				
$1\times\Delta\nu_{\text{cell}}$	0.286	0.987	1.000	0.790	0.019	0.105	0.096	0.105
$2\times\Delta\nu_{\text{cell}}$	0.286	0.953	1.000	0.762	0.020	0.144	0.102	0.144
$3\times\Delta\nu_{\text{cell}}$	0.286	0.934	1.000	0.747	0.026	0.188	0.131	0.188
$4\times\Delta\nu_{\text{cell}}$	0.286	0.934	1.000	0.747	0.035	0.215	0.174	0.215

culate[20] the hfs intensity ratios for these two cases. The results are displayed in Table IV.

Utilizing the data in Tables III and IV, $A(N_{\text{Rb}})$ was evaluated from Eq. (20) for a range of values of N_{Rb}. This was accomplished with another computer program which performed the integration over frequency. Thus we obtained a series of curves for the various lamp conditions assumed above. The two extremes, corresponding to case (a) line 4 and case (b) line 1 in Table IV, are displayed in Fig. 3 by dashed lines; the mean is shown as a solid line. It was found that case (a) and case (b) gave almost identical A versus N_{Rb} plots for the same Doppler width in the lamp. This indicates that the absorption is not very sensitive to the actual intensity ratios in the lamp. More important is the Doppler width in the lamp. Even so, a variation of this width by 1 to 4 times the Doppler width in the Rb cell produced extreme curves which, for a given value of A, represented about a ± 5% deviation in N_{Rb} from the mean.[21]

Hence we conclude that the density determination by this absorption technique is quite insensitive to the actual lamp conditions, providing reasonable care is exercised to eliminate extreme broadening and self-reversal. The solid curve in Fig. 3, which represents the mean of the extremes, is used as the theoretical A versus N_{Rb} curve to determine the density.

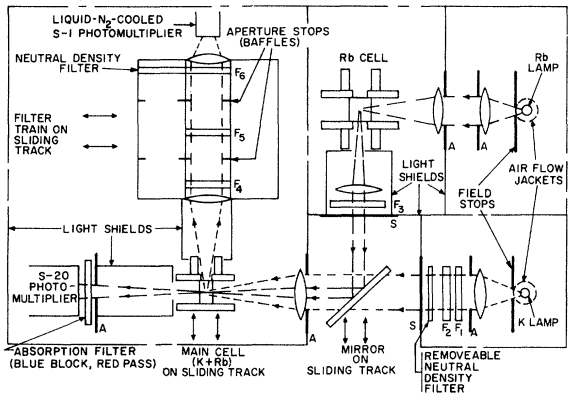

FIG. 4. Schematic diagram of the experiment: A = aperature stops; S = shutters; F_1 and F_2 = K-D1 (or D2) interference filters; F_3, F_4, F_5, F_6 = Rb-D1 interference filters.

B. Experimental Arrangement

The experimental procedure for the density determination is straightforward. A diagram of the apparatus is shown in Fig. 4. The Rb fluorescence cell, constructed of Pyrex, was cylindrical, 2 cm in diameter and 2 cm long. A sidearm of approximately 1 cm in diameter and 10 cm in length was attached to the underside. The Rb metal was transferred into the cell in the following manner. The Rb cell was first evacuated and baked at 200°C until a vacuum of 1×10^{-6} Torr was achieved, then an ampoule of Rb metal was broken and the metal distilled into the cell. The cell was further evacuated until a vacuum of 10^{-6} Torr was again obtained and the sidearm was then sealed off. The Rb cell was painted with aqua dag to reduce light scatter, taking special care to cover the edges of the entrance and exit windows. A copper tube (6 cm long) was wrapped around the cell. Apertures 1 cm in diameter were cut to form two side windows. Copper tubes 2 cm long were attached around each side window. The entire cell was wrapped with asbestos tape and chromel-alumel thermocouples were attached. The cell was further wrapped with asbestos tape and nichrome heating wire, extending down the sidearm as well, leaving approximately 3 cm at the bottom of the sidearm bare. The cell was then heated at 100°C for several days until all the metal had migrated to the bottom of the sidearm. A small heater was constructed by wrapping asbestos tape and nichrome wire around a tube of Pyrex which fitted snugly around the bottom of the sidearm. This allowed independent variation of

the sidearm temperature while maintaining the body temperature constant at 100°C.

The Rb resonance lamp was a conventional Osram lamp with the outer glass jacket removed. The lamp was painted with aqua dag leaving a 1-cm diameter aperture in the middle which formed the source window. The lamp was mounted upside down inside an air-flow jacket consisting of a cylindrical Pyrex Dewar with an air hose attached to the bottom. Cooling fins of copper were wrapped around the bottom of the lamp to prevent metal from coating the source window. The air-flow jacket allowed the operating temperature of the lamp to be varied. The appropriate lamp operating conditions were determined in the following manner.

In order to maintain a vapor pressure so that the optical depth in the Rb cell is less than one, the sidearm temperature of the Rb cell must be near room temperature. With the body of the Rb cell at 100°C and the sidearm at room temperature, absorption measurements were taken (at about 70% absorption in the main cell) for varying lamp temperatures. The absorption in the main cell and the fluorescence of the Rb cell were monitored as the lamp operating temperature was reduced. It was found that the absorption first increased rapidly and then leveled off with decreasing lamp operating temperature. (All absorption measurements were corrected for window absorption in the main cell by techniques described in the next section.) At the same time the Rb cell fluorescence was observed to increase by a factor of 40 and then gradually to decrease. The level region of absorption was maintained for a factor of 50 decrease in the Rb cell fluorescence. We interpret the initial rapid increase in absorption as due to the extreme broadening and self-reversal of the hot lamp (enclosed in the air flow jacket when no air was flowing). This is substantiated by the large increase in Rb cell fluorescence as the lamp was cooled.

The lamp operating conditions were adjusted for the level absorption region described above. Tests were then carried out on effects of the Rb vapor pressure in the Rb cell by varying the temperature of the sidearm. It was found that with the sidearm at room temperature, the Rb fluorescent radiation emerging from the side window of the Rb cell was negligibly self-reversed and had less than 1% residual scattered light from the lamp.[22] It is in the level region of absorption as a function of lamp temperature that we believe our density-measurement procedure is most valid. With these operating conditions our density determination was carried out.

IV. EXPERIMENTAL PROCEDURE AND RESULTS

The experimental arrangement is shown in Fig. 4. The K lamp was an Osram spectral lamp modified in the same way as the Rb lamp described in Sec. III, thus allowing us to vary its operating temperature. The lamp profile was adjusted to match the absorption profile in the main cell in order to provide the maximum useful signal.[23] The exciting K line was isolated with one or two interference filters,[24] each separating the two D lines with a leakage of less than one part in 10^3 for the unwanted component.

The main cell, constructed of Pyrex, was cylindrical (1 cm long and 2 cm in diameter) with two sidearms (1 cm in diameter and 10 cm long) attached to the bottom through a tube (4 mm in diameter and about 1 cm long). The cell was baked out, filled, sealed off, painted with aqua dag, and wrapped, all as described for the Rb cell, except that the main cell contained only one side window (6 mm long and 10 mm high). One sidearm contained Rb metal; the other contained K metal. A valve (glass-encased soft iron slug) allowed us to open or close the sidearm containing K metal, using a small magnet. Chromel-alumel thermocouples were attached at various positions on the main cell during wrapping. Thermocouples were also attached to the sidearms, whose temperatures could be varied independently from that of the main body by means of small heaters constructed as described in the previous section.

The main cell was mounted on a sliding track so that it could be accurately positioned to allow the light beam to pass through its center, or it could be removed from the path of the light beam as part of the absorption measurement for the Rb density determination. A sliding mirror (see Fig. 4) could be similarly positioned to allow either Rb or K light to pass through the main cell.

The fluorescence intensities were detected with an S-1 RCA 7102 photomultiplier, specially selected for high sensitivity. The photomultiplier was housed in a liquid-nitrogen–cooled Dewar[25] which reduced the dark current to 1×10^{-13} A at 1100 V. The K or Rb fluorescence signals were selected by interference filters mounted in cylinders on a sliding track inside a light-tight box (see Fig. 4) interposed between the main cell and the detector. The "cross-fluorescence" channel, for detecting Rb-sensitized fluorescence, contained either two or three Rb interference filters. Both filter combinations had a leakage of less than 5 parts in 10^6 for the undesired Rb component. (Potassium leakage is discussed later in this section.) The other channel in the filter train contained a neutral density filter for attenuating the K fluorescence signal, which was more than 6 orders of magnitude greater than the cross fluorescence. An S-20 photomultiplier in conjunction with a blue-blocking red-transmitting filter detected the Rb-D1 line used in the Rb density determination.

The output from both photomultipliers was displayed on a strip chart recorder used in conjunction with a Keithley 417 picoammeter. The design of the apparatus permitted rapid alternation between the density measurement and the K and Rb fluorescence measurements. This minimized systematic errors arising from slight nonequilibrium drifts in the vapor densities and from short-term fluctuations in the lamps. It is noteworthy that this experimental design allows the measurement of Rb density in exactly the same spatial region of the main cell in which the excitation transfer takes place.

The body of the main cell was maintained at 100°C during and between runs to minimize errors due to the saturation effects noted previously. The K concentration could be varied by opening the valve on the K sidearm and driving a small amount of K into the cell. The valve was then closed and the cell allowed to equilibrate for several days with the Rb sidearm at room temperature and the cell body at 100°C.

It was pointed out by Gallagher,[5] and subsequently found to be true in our system as well, that after the cell is allowed to equilibrate as described above, if the body temperature is suddenly reduced from 100°C to room temperature, the vapor densities in the cell will drop considerably below those corresponding to the room-temperature equilibrium vapor pressures, then gradually increase over a period of several days to the equilibrium values. This fact was used to advantage in the present experiment. Just prior to taking a run, the body temperature was reduced and the K fluorescence and Rb cross fluorescence, as well as the Rb absorption, were monitored as the cell cooled. All values leveled off and remained constant within experimental error as room temperature was approached. This technique permitted us to measure the residual scattered light (used to correct the fluorescence signals), and the window absorption of the main cell (used to correct the absorption measurement). At the lowest density data point in a run, the scattered light was about a 25% correction to the K fluorescence signal and was a correction of the order of the dark current to the Rb cross fluorescence signal.

We found experimentally that the K and Rb vapor densities in the main cell were proportional to each other (within experimental error) as the temperature of the Rb sidearm was varied from room temperature to 70°C during a run.[26] This fact is inferred from the linear plot of K fluorescence versus rubidium atom density shown in Fig. 5. This linearity was verified repeatedly to within 5% over the entire range 5×10^{10}–1×10^{12} Rb atoms/cm^3 for low K atom concentrations in the cell, and this proportionality between N_K and N_{Rb} was used as a consistency check on the other

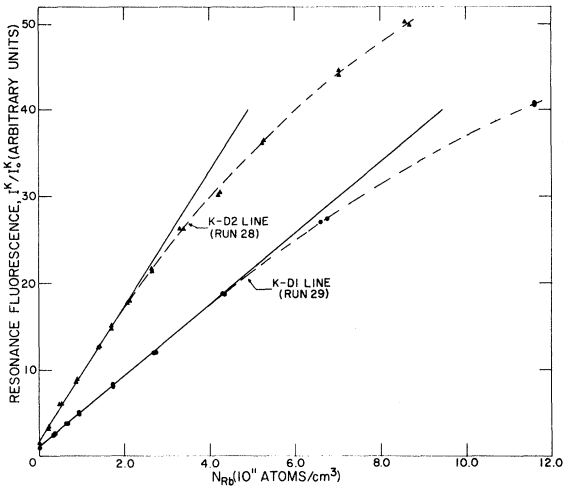

FIG. 5. Plots for two consecutive runs of the normalized potassium resonance fluorescence as a function of rubidium atom density (which we found experimentally to be proportional to the potassium-atom density). The data points on the vertical axis represent scattered light (see text).

data. To correct for slight drifts in lamp intensity (which amounted to about ±5% during a run) the fluorescence intensities were normalized by dividing by the incident signal measured with the S-20 photomultiplier through a neutral density filter with the main cell removed from the beam.

By extrapolating the linear plot in Fig. 5 to zero Rb density, a value was obtained for the residual scattered light. This value was found to agree within experimental error with the value obtained by the previously described technique of cooling the cell (given by the data point on the vertical axis of Fig. 5).

The window absorption in the main cell was also measured independently. A Cs lamp was placed at the position of the Rb lamp (see Fig. 4) and the Rb cell was replaced by a cell containing a colloidal gold suspension. The absorption in the main cell of the scattered Cs red lines agreed with the value obtained for the window absorption using the previous technique of cooling the cell.

The entire apparatus was thoroughly shielded against stray light and unwanted light signals. During a typical run (which was conducted in the dark) the window absorption and the scattered light were first measured as described above. Then, the body was reheated to 100° C and allowed to equilibrate. The Rb absorption and the I^K and I^{Rb} fluorescence intensities were then measured for various Rb sidearm temperatures in steps of about 5° from room temperature to 70°C. About 30 minutes was allowed between temperature changes in the sidearm to ensure steady-state equilibration.

Three criteria were used to establish the region

in which the K vapor was optically thin. First, as more K was added to the cell in subsequent runs, the plot of K fluorescence versus N_{Rb} was linear in the low-density regions and bent over toward higher densities. The linear region was assumed to correspond to optically thin conditions. Second, the plot of the fluorescence ratio I^{Rb}/I^{K} as a function of N_{Rb} was linear for low densities and bent upwards at higher densities, as the K radiation became trapped. This latter bend consistently occurred just slightly above the bend in the corresponding K fluorescence curve. This behavior was observed for runs taken with various K concentrations, thus substantiating the region in which K was optically thin. Finally, two complete series of runs were taken, each extending over a period of about a month. At the start of a given series of experimental runs, an oversupply of K was driven into the cell. Runs were then taken in three-to-four day intervals. It had been found that the K concentration in the cell gradually decreased as a function of time. A reasonably linear fit could be made to the I^{Rb}/I^{K} versus N_{Rb} plots, even in the early runs of a series. Nevertheless, it was apparent from the extreme curvature of the K fluorescence versus N_{Rb} plots that the K radiation was considerably trapped throughout these runs, and the cross sections so obtained using Eq. (2) were spuriously large, by as much as a factor of 4. As the K concentration continued to diminish in the cell, the apparent values of the cross section decreased in a systematic fashion, and toward the latter runs of a series the location of the valid linear region became evident from the bends in the two curves. Cross sections calculated in this linear region agreed to about ± 10%. Although a direct determination of the K vapor density was not made, it can be roughly estimated to be $\lesssim 5\times10^{10}$ atoms/cm^3 from the onset of nonlinearity in the K and Rb D1 fluorescence curves (Figs. 5 and 6).

Figure 5 shows the potassium resonance fluorescence curves for two consecutive runs taken in the latter stages of one of the series and illustrates the departures from linearity when K radiation starts to become trapped. These departures occur in the reciprocal ratio of the f values for the potassium D1 and D2 lines. The ratio of the slopes also satisfies the proper dependence.

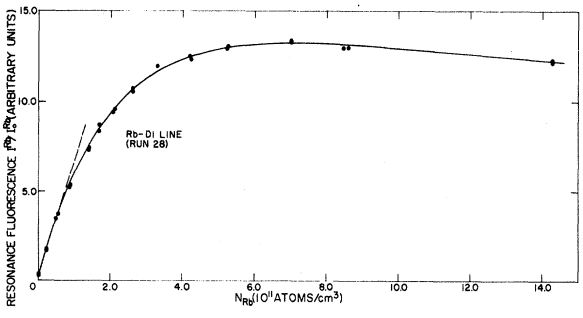

FIG. 6. Plot of the normalized rubidium resonance fluorescence from the main cell as a function of rubidium-atom density. The data point on the vertical axis represents scattered light (see text).

Figure 7 shows the corresponding I^{Rb}/I^{K} fluorescence ratio measured as a function of Rb atom density for the same two runs as shown in Fig. 5. The nonzero intercepts of the curves in Fig. 7 are due to K fluorescence leakage through the Rb interference filters. For the K-D2 line the leakage was about 2 parts in 10^7 for the two-filter combination and 5 parts in 10^8 for the three-filter combination. The K-D1 leakage was about a factor of 2 worse. The actual intercept is the ratio of K to Rb fluorescence transmission. These rejection ratios were independently measured and agreed within experimental error with the values determined from the intercepts. This leakage, although substantial at the low densities necessary to ensure the absence of radiation trapping, did not affect the slope of the curves from which the cross sections were obtained, and hence was not subtracted from the data. Note that in Fig. 7 the departures from linearity again show the anticipated dependence on the f values for the two K lines involved. The deviations in Fig. 7 consistently occur slightly above the corresponding deviations in Fig. 5.

Table V lists the cross sections obtained for the two alkali-atom excitation-transfer processes we studied. The values quoted are averages of five experimental runs for $Q(K^2P_{3/2}\rightarrow Rb^2P_{1/2})$ and three experimental runs for $Q(K^2P_{1/2}\rightarrow Rb^2P_{1/2})$, all taken in the linear region where K radiation was not trapped. These values all agreed with each other to about ± 10% for the former and ± 15% for the latter. We were unable in this study to determine cross sections for excitation transfer to the Rb $^2P_{3/2}$ level owing to too much light leakage through our filter system, but efforts are underway to make these measurements possible.

V. ERROR ANALYSIS

A. Radiation Trapping

The experimental checks used to ensure the absence of potassium-radiation imprisonment have already been discussed. Several arguments can be advanced to show that rubidium-radiation trapping was a minor source of error. First, some runs extend down to a Rb optical depth of 0.1 and others to as high as 2.0. The cross sections calculated from all these runs gave the same value to about ± 10%. Second, the incident K beam was imaged down to one-fifth the diameter of the main cell, and scanned from the center of the cell to

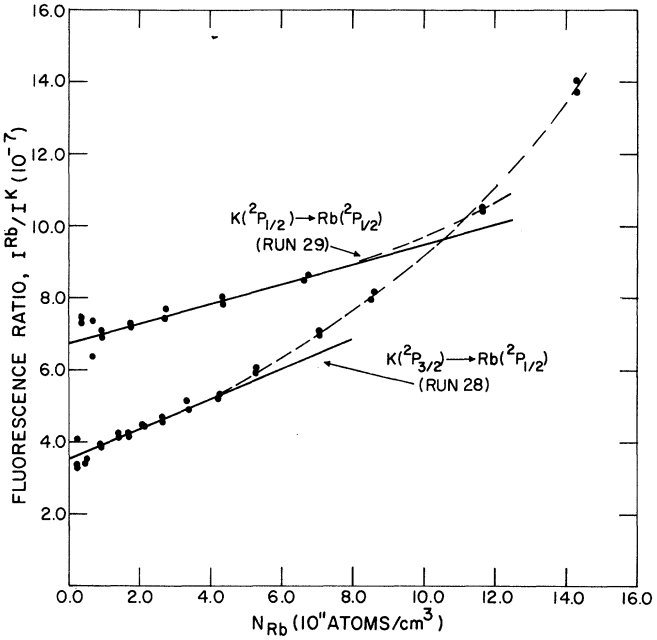

FIG. 7. Ratio of Rb cross fluorescence to K resonance fluorescence detected at right angles to the exciting K-D2 (or D1) beam for the same two consecutive runs shown in Fig. 5. The intercept is due to K leakage through the Rb-D1 interference filters of the detection system. A weighted least-squares fit was made to the points in the linear region as described in the text.

the edge of the exit window by moving the cell back on the sliding track. The I^{Rb}/I^{K} fluorescence ratio was found to differ with position by less than 20% at the highest Rb densities (1×10^{12} atom/cm^3) and by much less at lower densities. The K vapor was optically thin for these tests. The diameter of the K beam used in our runs was normally one-half the diameter of the cell, and we conclude that Rb-radiation trapping did not contribute appreciable error at the Rb densities for which our cross section was measured. Finally, cross-section measurements were originally taken for Rb densities about a factor of 30 larger (using absorption of the blue lines of Rb for the density determination) and a corresponding K concentration about a factor of 30 smaller. The values of the cross sections under these conditions were only about a factor of 2 too small.

B. Spectral Purity

The leakage of potassium light through the Rb interference filters was discussed in Sec. IV. Dark current, black-body radiation, and residual light were subtracted for each data point by blocking the incident K beam with a shutter (see Fig. 4). These stray signals, along with the K leakage, contributed considerable scatter to the low-density data but were less important at higher densities. A least-squares fit, weighted by the reciprocal squares of the estimated uncertainty in each data point, was made to the linear region of the plot (see Fig. 7).

The transmission of the Rb filter combination to the Rb fluorescent light and the transmission of the neutral density filter to the potassium fluorescent light were measured *in situ* by using fluorescence excited in the main cell under optically thin conditions. This procedure minimized systematic errors from geometrical effects, but not without several percent uncertainty due to the angular dependence of the transmission.

The separation of the K-D lines in the incident beam was achieved by using one or two K interference filters, each with a transmission of the undesired K component of less than one part in 10^3. A more important concern was the possible Rb contamination in the K lamp. With one K filter the Rb contamination in the beam was determined to be less than 1 part in 10^9. As a check, a second K filter was inserted in the beam. The use of two K filters yielded the same cross section as one, indicating that direct Rb fluorescence excited by the incident beam was negligible. Moreover, such an error would not yield the linear dependence we found in Fig. 7.

C. Molecular Fluorescence

The question arises as to what extent band emission from the molecular species K_2, RbK, and Rb_2 leaking through the approximately 50 Å halfwidths of the Rb interference filters can contribute to the measured signal I^{Rb}. The band structure of these molecules is poorly known.[27] If the incident K line excited fluorescence in these species, it would give the same density dependence as the cross fluorescence signal since we found experimentally that N_{Rb} was proportional to N_K in our cell. This potential source of error was easily checked (and found to be negligible) by inserting a rubidium vapor absorption cell between

TABLE V. Absolute cross sections for excitation transfer from potassium to rubidium. ($T = 365°K \pm 2\%$) The reaction rate is defined here as $Q\bar{v}$.

Excitation Transfer Process	Cross section (Å^2)	Reaction rate (cm^3/sec)
$K(^2P_{3/2}) \rightarrow Rb(^2P_{1/2})$	$2.6 \pm 20\%$	$1.4 \times 10^{-11} \pm 20\%$
$K(^2P_{1/2}) \rightarrow Rb(^2P_{1/2})$	$2.2 \pm 25\%$	$1.2 \times 10^{-11} \pm 25\%$

the main cell and the detector. For various densities in the Rb absorption cell, we found that the same percentage of the cross fluorescence was absorbed as Rb resonance fluorescence excited in the main cell by Rb light. This test, in conjunction with the purity of the exciting K beam, served as an important consistency check confirming that we were, in fact, observing only sensitized fluorescence.

D. Molecular Impurities

Potassium and rubidium intramultiplet transfer cross sections for collisions with molecular gases, such as N_2, are of the order of those with the alkalies themselves.[28] In Sec. IV we described our procedure for transferring high-purity alkali metals[29] into the cells, in which the cells were tipped off under a vacuum of 10^{-6} Torr. At no time in the main cell's history was there any evidence of foreign-gas contamination. Hence mixing between tha alkali doublets due to such impurities is believed to be negligible. At the alkali-atom pressures we used the alkali dimer concentrations[30] could not contribute to the signal by these means.

E. Velocity Dependence of the Cross Section

Equation (6) shows that the cross section we measure is an average of the velocity-dependent cross section $\sigma(v)$ over the relative velocity distribution of the colliding partners. The velocity dependence of the cross sections for excitation transfer from one alkali atom to another has not been measured. Two sources of error are then possible, (a) non-Maxwellian velocity selection of the K* atoms due to the profile of the incident beam and (b) temperature gradients in the main cell.

If the exciting light had a uniform intensity across the absorption profile (white light excitation), then the excited-state velocity distribution function would be the same as the ground-state distribution. For the conditions of our experiment, the incident K-light profile was adjusted to maximize the useful signal, and the nonthermal velocity selection of the K atoms in one direction had a small effect on the relative collision velocity distribution. This source of error should be neglibible, as was indeed found by Gallagher[5] under similar conditions.

Temperature variations across the main cell were measured and the center of the windows was found to be about 15° cooler than the walls of the cell. All temperatures in the main cell were constant to better than ±1 degree, and in the sidearms to ±0.3 of a degree. It should be noted that our cross sections are average cross sections for $T = 365°K$ (±2%).

F. Density Measurement

Errors in the density measurement arise primarily from deviation in the experimental line profile from the assumed profile used in the theoretical analysis. The theoretical and experimental checks appear to dismiss any large error here, but several percent uncertainty is reasonable. Errors in the absolute temperature contribute about 2% uncertainty. The length of the main cell (inner dimension)[31] was known to better than 1%, and the slight nonparallelism of the beam, which amounted to a maximum divergence of approximately 4° at the detector, produces negligible additional error in the optical path length. Errors associated with the window-absorption correction, slight drifts in the cell's vapor pressures and in the lamp's intensity add a few percent uncertainty. The over-all error in the density measurement is estimated as ±10%.

G. Spectral Response of the Detection System

The S-1 cathode of the photomultiplier has a nearly flat spectral response over the range 7600 to 8000 Å. No correction was made for the change in quantum efficiency between the K and Rb wavelengths, which adds a few percent uncertainty to the I^{Rb}/I^{K} ratios.

H. Polarization Corrections

The exciting beam in our experiment was unpolarized and the detection optics were insensitive to polarization. However, excitation by a unidirectional beam causes alignment of the atoms in the excited state. The fluorescence observed at right angles to the beam direction is somewhat polarized for a $^2P_{3/2}$ state but unpolarized for a $^2P_{1/2}$ state.[1] The polarization was measured and introduced a correction which lowered the cross section $Q(K\ ^2P_{3/2} \rightarrow Rb\ ^2P_{1/2})$ by 5% from that given by the measured intensity ratio in Fig. 7.

The cross sections we measured are averages over all the individual Zeeman transitions. The

cells were heated by current (≈ 1 A) flowing through bifilar windings. The magnetic field at the location of the cells, including the earth's field, was about 1 G and produced negligible Zeeman scanning of the magnetic sublevels of the atoms.[32]

I. Conclusion

The cross sections are shown in Table V with their estimated errors. The $K\,^2P_{1/2} \rightarrow Rb\,^2P_{1/2}$ data were less accurate than the $K\,^2P_{3/2} \rightarrow Rb\,^2P_{1/2}$ data because for the former there was greater K leakage through the Rb filters and smaller fluorescence signals. We have assigned an accuracy of $\pm 20\%$ for $Q(K\,^2P_{3/2} \rightarrow Rb\,^2P_{1/2})$ and $\pm 25\%$ for $Q(K\,^2P_{1/2} \rightarrow Rb\,^2P_{1/2})$, well in excess of measured fluctuations.

Note added in proof: Since this work was submitted we have learned of the recent investigation of the K*+Rb collision system by E. S. Hrycyshyn and L. Krause, Can. J. Phys. 47, 215 (1969). They report cross section of $Q(K\,^2P_{1/2} \rightarrow Rb\,^2P_{1/2}) = 2.7 \pm 0.6$ Å^2 and $Q(K\,^2P_{3/2} \rightarrow Rb\,^2P_{1/2}) = 1.9 \pm 0.6$ Å^2 based on a quite different density-determination procedure. Within the stated experimental errors their cross sections and our cross sections are in agreement with each other.

ACKNOWLEDGMENTS

We are indebted to Dr. Alan Gallagher and to Dr. Peter L. Bender for numerous useful and stimulating discussions through the course of this study. The authors are pleased to acknowledge the close collaboration of Dr. John K. Link in the early stages of this work.

APPENDIX

We outline[20] below the derivation of Eqs. (21) and (22) used in the density determination. The f value for $F \rightarrow F'$ is related to the transition probability per sec by

$$f_{F \rightarrow F'} = \frac{c}{8\pi^2 \nu_0^2 r_0} \frac{2F'+1}{2F+1} A_{F' \rightarrow F}. \tag{A1}$$

Since

$$A_{F' \rightarrow F} = \frac{1}{2F'+1} \sum_{M_{F'}, M_F} A_{F'M_{F'} \rightarrow FM_F}, \tag{A2}$$

where

$$A_{F'M_{F'} \rightarrow FM_F} = \frac{64\pi^4 e^2 \nu_0^3}{3hc^3} \frac{1}{2F'+1} \times [C(F1F'; M_F, M_{F'} - M_F, M_{F'})]^2 \times |(J'IF'||r^{(1)}||JIF)|^2, \tag{A3}$$

it follows that

$$A_{F' \rightarrow F} = \frac{64\pi^4 e^2 \nu_0^3}{3hc^3} \frac{1}{2F'+1} \times |(J'IF'||r^{(1)}||JIF)|^2. \tag{A4}$$

The double-barred matrix element is in the usual notation of Racah.[33] Racah's methods can be used to reduce the matrix element in (A4) giving

$$A_{F' \rightarrow F} = (64\pi^4 e^2 \nu_0^3 / 3hc^3)(2F+1) \times [W(J'F'JF; I1)]^2 |(J'||r^{(1)}||J)|^2. \tag{A5}$$

From Eqs. (A1) and (A5) it follows that

$$f_{F \rightarrow F'} = \gamma_1 (2F'+1) [W(J'F'JF; I1)]^2, \tag{A6}$$

where γ_1 is a constant. Equation (A6) is the same as Eq. (21) in the text.

The f sum rule in Eq. (22) is derived as follows. Since

$$A_{J' \rightarrow J} = \frac{\sum_{F', F} (2F'+1) A_{F' \rightarrow F}}{\sum_{F'} (2F'+1)}, \tag{A7}$$

Eqs. (A5) and (A7) may be combined to yield

$$A_{J' \rightarrow J} = \frac{\gamma_2}{(2J'+1)} |(J'||r^{(1)}||J)|^2, \tag{A8}$$

where γ_2 is a constant. We also obtain with the help of Eq. (A5) the relation

$$\sum_{F'} (2F'+1) A_{F' \rightarrow F} = \gamma_2 \frac{2F+1}{2J+1} |(J'||r^{(1)}||J)|^2. \tag{A9}$$

Equations (A8) and (A9) may be combined to give

$$A_{J' \rightarrow J} = \frac{2J+1}{2J'+1} \sum_{F'} \frac{2F'+1}{2F+1} A_{F' \rightarrow F}. \tag{A10}$$

The total f value for the fine-structure transition is given by

$$f_{J \rightarrow J'} = \frac{c}{8\pi^2 \nu_0^2 r_0} \frac{2J'+1}{2J+1} A_{J' \rightarrow J}. \tag{A11}$$

Equations (A1), (A10), and (A11) are then used to establish the desired relation

$$f_{J \rightarrow J'} = \sum_{F'} f_{F \rightarrow F'}, \tag{A12}$$

of which Eq. (22) is a special case.

*This work was supported in part by the National Science Foundation and in part by the Advanced Research Projects Agency of the Department of Defense under the Strategic Technology Office. A preliminary account was reported in Bull. Am. Phys. Soc. 12, 1147 (1967).

†National Defense Education Act Predoctoral Fellowship 1965–1968; National Science Foundation Traineeship 1968–1969.

‡Alfred P. Sloan Fellow.

[1]A. C. G. Michell and M. W. Zemansky, Resonance Radiation and Excited Atoms (Cambridge University Press, Cambridge, England, 1961).

[2]P. Pringsheim, Fluorescence and Phosphorescence (Interscience Publishers, Inc., New York, 1949).

[3]J. G. Winans, Rev. Mod. Phys. 16, 175 (1944).

[4]L. Krause, Appl. Opt. 5, 1375 (1966).

[5]A. Gallagher, Phys. Rev. 172, 88 (1968).

[6]A. Javan, Phys. Rev. Letters 3, 87 (1959); W. R. Bennett, Jr., A. Javan, and E. A. Ballik, Bull. Am. Phys. Soc. 5, 496 (1960).

[7]J. K. Link, J. Opt. Soc. Am. 56, 1195 (1966).

[8]G. D. Chapman and L. Krause, Can. J. Phys. 44, 753 (1965).

[9]A. G. A. Rae and L. Krause, Can. J. Phys. 43, 1574 (1965).

[10]It might be thought that the influence of Rb-radiation trapping on the experiment could be reduced by making the exciting beam almost graze the side of the cylindrical cell. Although this procedure minimizes the Rb-radiation trapping, it does not minimize the change of the I_1^{Rb}/I_2^{K} ratio. The potassium radiation for optically thin conditions radiates cylindrically symmetrically about the exciting beam axis; the rubidium radiation under somewhat trapped conditions radiates preferentially in the direction of the detector when the exciting beam grazes the window.

[11]G. S. Hayne, E. S. Ensberg, and H. G. Robinson, Phys. Rev. 171, 20 (1968); L. C. Balling, Phys. Rev. 151, 1 (1966).

[12]S. M. Jarrett, Phys. Rev. 133, A111 (1964); Ph. D. thesis, University of Michigan, 1962 (unpublished).

[13]M. Rozwadowski and E. Lipworth, J. Chem. Phys. 43, 2347 (1965).

[14]H. M. Gibbs and R. J. Hull, Phys. Rev. 153, 132 (1967); H. M. Gibbs, Ph. D. thesis, University of California Lawrence Radiation Laboratory Report No. UCRL-16034, 1965 (unpublished).

[15]This statement is valid if the dominant broadening mechanism is due to the Doppler effect, as was the case for the alkalies in our experiment. Note that the motion along the beam direction is uncoupled from the motion at right angles. See Ref. 1, pp. 106–110.

[16]B. Bederson and V. Jaccarino, Phys. Rev. 87, A228 (1952).

[17]B. Senitsky and I. I. Rabi, Phys. Rev. 103, 315 (1956).

[18]H. Kopfermann and H. Krüger, Z. Physik 103, 485 (1936).

[19]R. B. Leighton, Principles of Modern Physics (McGraw-Hill Book Co., Inc., New York, 1959), Appendix G.

[20]For details see M. H. Ornstein, Ph. D. thesis, University of Colorado, Boulder, Colo., 1969 (unpublished).

[21]In the unrealistic case that the lamp profile can be approximated by white light, it was found that the density, as determined from the plot of A versus N_{Rb}, was less than 20% larger than the solid curve (mean) in Fig. 3.

[22]Another advantage of this technique for determining the density is that the Rb fluorescence cell effectively filters the light from the Rb lamp removing nearby weak lines (due to argon) which would be passed by the Rb interference filter.

[23]The useful light obtained from our air-cooled Osram lamp, as determined by the K fluorescence of the main cell, is as intense as what we obtained by driving the lamp by microwave excitation.

[24]The potassium interference filters were made to order by Thin Film Products Co., 169 Bridge St., Cambridge, Mass., with a half-width of about 5 Å.

[25]We thank Dr. Arthur L. Schmeltekopf, Environmental Science Services Administration, Boulder, Colo., for providing us with his plans for the design of the Dewar.

[26]This effect is not obvious *a priori* but was verified repeatedly. This linearity is in fair agreement with the predictions based on Raoult's law.

[27]G. Herzberg, Molecular Spectra and Molecular Structure: I. Spectra of Diatomic Molecules (D. Van Nostrand Co., Inc., Princeton, New Jersey, 1950).

[28]D. A. McGillis and L. Krause, Can. J. Phys. 46, 25 (1968); 46, 1051 (1968); Phys. Rev. 153, 44 (1967). M. Stupavsky and L. Krause, Can. J. Phys. 46, 2127 (1968).

[29]Our alkalies (99.995% stated purity) were obtained from Penn Rare Metals, Kawecki Chemical Co., Revere, Pa., in sealed ampoules.

[30]M. Lapp and L. P. Harris, J. Quant. Spectry. Radiative Transfer 6, 169 (1966).

[31]The cell was constructed using a carbon block jig to ensure parallelism of the windows.

[32]See W. Berdowski and L. Krause, Phys. Rev. 165, 158 (1968).

[33]G. Racah, Phys. Rev. 62, 438 (1942).